

## Emissive sheath measurements in the afterglow of a radio frequency plasma

J. P. Sheehan, E. V. Barnat, B. R. Weatherford, I. D. Kaganovich, and N. Hershkowitz

Citation: *Physics of Plasmas* (1994-present) **21**, 013510 (2014); doi: 10.1063/1.4861888

View online: <http://dx.doi.org/10.1063/1.4861888>

View Table of Contents: <http://scitation.aip.org/content/aip/journal/pop/21/1?ver=pdfcov>

Published by the [AIP Publishing](#)

---

### Articles you may be interested in

[Negative plasma potential in a multidipole chamber with a dielectric coated plasma boundary](#)

*J. Vac. Sci. Technol. A* **30**, 031302 (2012); 10.1116/1.4705514

[Measurement of plasma-surface energy fluxes in an argon rf-discharge by means of calorimetric probes and fluorescent microparticles](#)

*Phys. Plasmas* **17**, 113707 (2010); 10.1063/1.3484876

[Time-resolved measurements of the E -to- H mode transition in electronegative pulse-modulated inductively coupled plasmas](#)

*J. Vac. Sci. Technol. A* **24**, 2151 (2006); 10.1116/1.2359736

[Time evolution of electron energy distribution function and plasma parameters in pulsed and unbalanced magnetron argon discharge](#)

*J. Appl. Phys.* **98**, 043301 (2005); 10.1063/1.1990264

[Ion kinetic effects in radio-frequency sheaths](#)

*Phys. Plasmas* **12**, 033505 (2005); 10.1063/1.1857915

---



### Vacuum Solutions from a Single Source

- Turbopumps
- Backing pumps
- Leak detectors
- Measurement and analysis equipment
- Chambers and components

**PFEIFFER**  **VACUUM**

# Emissive sheath measurements in the afterglow of a radio frequency plasma

J. P. Sheehan,<sup>1,a)</sup> E. V. Barnat,<sup>2</sup> B. R. Weatherford,<sup>2</sup> I. D. Kaganovich,<sup>3</sup> and N. Hershkowitz<sup>1</sup>

<sup>1</sup>*Nuclear Engineering and Engineering Physics, University of Wisconsin—Madison, Madison, Wisconsin 53706, USA*

<sup>2</sup>*Sandia National Laboratories, Albuquerque, New Mexico 87185, USA*

<sup>3</sup>*Princeton Plasma Physics Laboratory, Princeton, New Jersey 08540, USA*

(Received 29 October 2013; accepted 23 December 2013; published online 30 January 2014)

The difference between the plasma potential and the floating potential of a highly emissive planar surface was measured in the afterglow of a radio frequency discharge. A Langmuir probe was used to measure the electron temperature and an emissive probe was used to measure the spatial distribution of the potential using the inflection point in the limit of zero emission technique. Time-resolved measurements were made using the slow-sweep method, a technique for measuring time-resolved current-voltage traces. This was the first time the inflection point in the limit of zero emission was used to make time-resolved measurements. Measurements of the potential profile of the presheath indicate that the potential penetrated approximately 50% farther into the plasma when a surface was emitting electrons. The experiments confirmed a recent kinetic theory of emissive sheaths, demonstrating that late in the afterglow as the plasma electron temperature approached the emitted electron temperature, the emissive sheath potential shrank to zero. However, the difference between the plasma potential and the floating potential of a highly emissive planar surface data appeared to be much less sensitive to the electron temperature ratio than the theory predicts. © 2014 AIP Publishing LLC. [<http://dx.doi.org/10.1063/1.4861888>]

## I. INTRODUCTION

How electron emission affects the plasma sheath is an important phenomenon in a wide variety of laboratory plasma devices. Secondary electron emission from Hall thruster channel walls plays a significant role in Hall thruster operation by modifying the sheath.<sup>1</sup> Many investigations of low temperature discharges use emissive probes to measure the plasma potential.<sup>2</sup> In tokamaks, significant secondary electron emission from divertor tiles can have a profound impact on the heat flux to those surfaces<sup>3</sup> and miscalculating the heat flux can lead to severe damage caused by unexpected particle fluxes. Developing a comprehensive understand of emissive sheaths is important for all of these applications.

Electron emission from a surface significantly affects the sheath surrounding that surface by reducing the net space-charge in the sheath.<sup>4</sup> The emitted electrons reduce the sheath potential as well as the electric field at the surface. With enough emission current, the sheath becomes space-charge limited and a virtual cathode, a non-monotonic minimum in the potential profile, forms near the surface.<sup>5,6</sup> In space-charge limited emission, the sheath potential is approximately  $T_{ep}/e$  (where  $T_{ep}$  is the plasma electron temperature in eV), significantly smaller than the collecting sheath potential of  $3 - 5T_{ep}/e$ . This fact can be used to approximate the electrostatic potential as the floating potential of a highly emissive probe, often called the floating point technique for emissive probes.<sup>7,8</sup> While there is an error in this measurement on the order of an electron temperature, it is often ignored or assumed to be small.

The often used fluid theory of emissive sheaths<sup>4</sup> assumes a planar, one dimensional geometry where the plasma

electrons have a Maxwellian distribution, the ions are cold and accelerated to the sheath edge to fulfill Bohm's criterion,<sup>9,10</sup> and the emitted electrons begin with zero energy. This is a collisionless theory. The plasma electrons are assumed to follow the Boltzmann relation, which assumes that the flux of electrons that reach the surface is small compared to the flux that enters the sheath and is reflected back out. By solving Poisson's equation, it was determined that the sheath potential (the potential difference between the sheath edge and the surface) of a planar emissive surface in space-charge limited emission is  $1.02T_{ep}/e$ . This analysis of emissive sheaths was generalized for non-floating surfaces<sup>11</sup> and for non-Maxwellian plasma Electron Velocity Distribution Functions (EVDf's).<sup>12</sup> A kinetic theory of the emissive sheath problem was formulated to account for the effect of ion mass and temperature.<sup>13,14</sup> Rather than a presheath, a "source sheath" (a double layer structure to accelerate ions) was assumed to better match the particle-in-cell simulations. While that theory captured some kinetic effects, it did not account for the effects of the emitted electron temperature.

Very few emissive sheath potential measurements have been made. Measurements in a Hall thruster indicated that the difference between the plasma potential and floating potential of a highly emitting probe was  $\sim 2T_{ep}/e$ .<sup>8</sup> In several experiments, sheath potential measurements were made near a hot cathode or a surface with a high secondary electron emission coefficient and virtual cathodes were observed, but temperature effects have not been investigated.<sup>5,6,15</sup> This article reports experiments which measured the potential of both collecting and emissive sheaths in the afterglow of a pulsed radio frequency (RF) plasma. Time-resolved measurements allowed measurements of the sheath potential for a range of electron temperatures.

<sup>a)</sup>Electronic mail: sheehan@umich.edu

## II. KINETIC THEORY OF EMISSIVE SHEATHS

Recently, a kinetic theory of the sheath surrounding electron emitting surfaces was reported.<sup>16</sup> It improves upon the well-known fluid theory of emissive sheaths<sup>4</sup> by accounting for the velocity distribution functions of the plasma and emitted electrons. In the fluid theory, the Boltzmann relation was used to determine the plasma electron density as a function of potential in the sheath. For emissive sheaths, which have smaller potentials than collecting sheaths, a significant fraction of plasma electrons entering the sheath reach the surface, violating assumptions implicit in the Boltzmann relation. The kinetic theory assumed that the plasma electrons in the bulk had a Maxwellian distribution and accounted for plasma electrons lost to the surface which modified the EVDF in the sheath. The fluid theory also neglects the energy distribution of emitted electrons, which is a half-Maxwellian equal to the surface temperature for thermionic emission<sup>17</sup> and a more complex function for secondary electron emission.<sup>18</sup> In the kinetic theory, the electrons were assumed to be emitted with a half-Maxwellian which simplified the analytic treatment.

The emissive sheath potential was defined as the potential difference between the sheath edge (where the ions fulfill Bohm's criterion) and the surface when the sheath was marginally space-charge limited. To determine the emissive sheath potential, Poisson's equation was solved with Bohm's criterion modified to account for the emitted electrons. The emissive sheath potential normalized to the plasma electron temperature as a function of the plasma electron temperature to emitted electron temperature ratio ( $\Theta_e$ ) is shown in Fig. 1.<sup>16</sup> On the far right of the graph, in the limit as the emitted electron temperature goes to zero or the plasma electron temperature becomes large, the sheath potential is slightly smaller than the fluid theory prediction due to the effect the electrons lost to the surface have on the sheath. The major effect on the emissive sheath, however, comes from the emitted electron temperature. As the plasma electron temperature approaches the emitted electron temperature the sheath potential shrinks drastically, going to zero as the plasma electron temperature equals the emitted electron temperature. Only by considering both the distributions of the emitted electrons and the plasma electrons can this effect

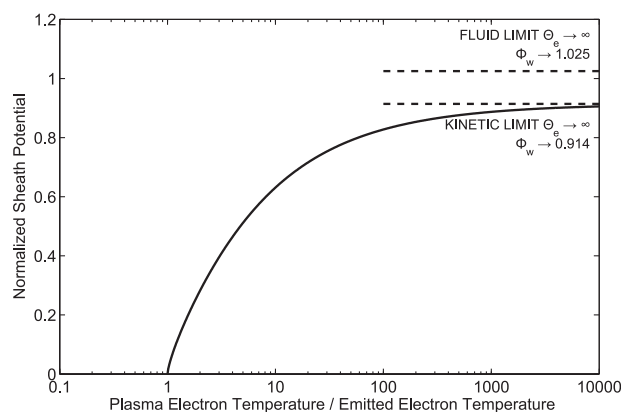


FIG. 1. Normalized emissive sheath potential versus plasma electron temperature to emitted electron temperature ratio.

be accurately captured. These predictions were in good agreement with particle-in-cell simulations.<sup>16</sup>

## III. EXPERIMENTAL SETUP

The experiments to test the kinetic theory of the emissive sheath were performed in a modified version of the Gaseous Electronics Conference (GEC) reference cell.<sup>19,20</sup> The vacuum chamber was a cylinder 22.3 cm long and 25.1 cm in diameter. The working gas was helium and the neutral pressure was 25 mTorr. At the top port of the vacuum chamber was a Pyrex dome around which a copper antenna was wrapped to capacitively couple 30 W of 10 MHz RF power into the plasma. The RF signal was pulsed at a rate of 60 Hz, turning the power off for 2.5 ms during which time measurements were made.

A cylindrical cathode was surrounded by a co-planar, annular electrode, as shown in Fig. 2. The outer, annular electrode was made of stainless steel and was grounded. The inner electrode was a 2.54 cm diameter electron emitting cathode made of barium doped tungsten (a HeatWave Labs, Inc. TB-198) and was heated with a DC current, driving thermionic emission of electrons from the surface. It was determined that 10.5 A of current, which heated the cathode to  $\sim 900^\circ\text{C}$ , kept the sheath in space-charge limited emission for the entire afterglow. The cathode color in Fig. 2 comes from its glow due to heating. While emissive probes made of thoriated tungsten typically glow white hot before they begin to emit, the planar emitter operated at a lower temperature and had a relatively faint orange glow when emitting. The surface of the emitter and that of the annular electrode were electrically isolated and the floating potential of each could be measured.

An emissive probe and a Langmuir probe were used to make measurements of the plasma potential and electron temperature in the afterglow. The Langmuir probe was made of tungsten wire with a length of 0.95 cm and a diameter of  $250\ \mu\text{m}$ . The emissive probe was a hairpin loop<sup>2,7</sup> of thoriated tungsten, approximately 1 cm long and  $76\ \mu\text{m}$  in diameter. The shafts of both probes were shielded with a stainless steel tube to reduce stray capacitance and suppress the displacement currents which disrupted the probe measurements in the afterglow. Both probes were positioned 3 cm above

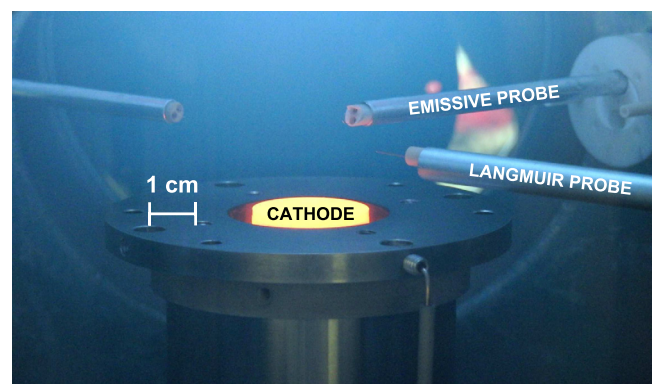


FIG. 2. A photo of the electrodes, Langmuir probe, and emissive probe in the modified GEC reference cell. The heated cathode is glowing orange in this image.

the electrodes. The probe in the right foreground was the Langmuir probe and the one in the right background was the emissive probe.

Making time-resolved probe measurements in the afterglow requires special considerations for the probe circuit, shown in Fig. 3. To measure the electron temperature with the Langmuir probe and the plasma potential with the emissive probe, it was necessary to measure current-voltage (I-V) characteristics, which this circuit allowed.<sup>21,22</sup> The variable power supply provided the sweep voltage ( $V_{\text{VAR}}$ ) while an additional floating power supply offset that bias by  $-15\text{ V}$  so the probe could be swept from negative to positive voltages with respect to ground. The inductors and capacitors were included to reduce RF fluctuations in the probe current. The emissive probe was heated with a DC current ( $I_H$ ) of  $\sim 0.8\text{ A}$  and the bias on the probe was measured as the bias in the middle of the filament. The probe current was determined by measuring the current across the  $10\text{ k}\Omega$  shunt resistor using a 50:1 differential probe. This same circuit was used for Langmuir probe measurements, but only one of the probe legs was connected and no heating current was used.

#### IV. SLOW-SWEEP PROBE METHOD

One method for making time-resolved I-V trace measurements is to sweep the probe quickly as compared to the temporal event to be measured. This is known as the fast-sweep probe method and can be difficult to execute due to technical and physical limitations.<sup>23-25</sup> The fast-sweep method has the benefit of being able to capture non-repeatable events. If, however, the temporal response being measured is periodic, the slow-sweep probe method has

good accuracy with a simpler setup.<sup>26-28</sup> To execute this method, the probe is biased at a constant potential and current is measured as a function of time. That procedure is performed for a range of bias voltages, and by transposing the data, probe current versus bias voltage at various times can be obtained. If used in conjunction with a boxcar averager, the I-V trace can be measured in a certain window of time,<sup>29</sup> but the benefit of measuring the current for all times is the I-V trace at every time is collected in one set of measurements.

The slow-sweep method was used for both the Langmuir probe and emissive probe. Examples of emissive probe I-V traces are shown in Fig. 4. One can observe how the inflection point (indicative of the plasma potential) becomes less positive later in the afterglow. The bulk plasma potential (the plasma potential far from any surface) was measured using the inflection point in the limit of zero emission technique.<sup>2,22</sup> This technique involves measuring the I-V trace for a variety of low emission currents (far below the space-charge limit) and extrapolating the inflection point to where the emission current is zero. The inflection point in the limit of zero emission technique has a predicted accuracy of  $T_{ep}/10e$ , much smaller than the  $T_{ep}/e$  error of the floating potential in the limit of large emission technique.<sup>8</sup> Until now, the inflection point technique was limited in that it could not be used to measure time-varying plasma potentials with frequencies larger than  $\sim 1\text{ kHz}$ . The thermalization time needed to stabilize the probe temperature in between I-V traces is the major limiting factor, which is unique to the inflection point technique. In combination with the slow-sweep probe method, though, those measurements are now possible and will allow

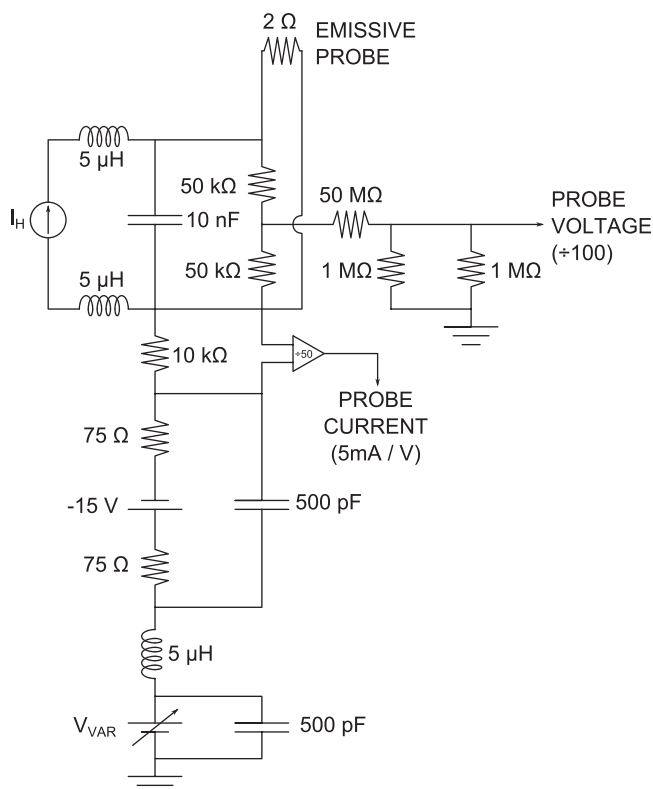


FIG. 3. Probe circuit for measuring I-V traces.

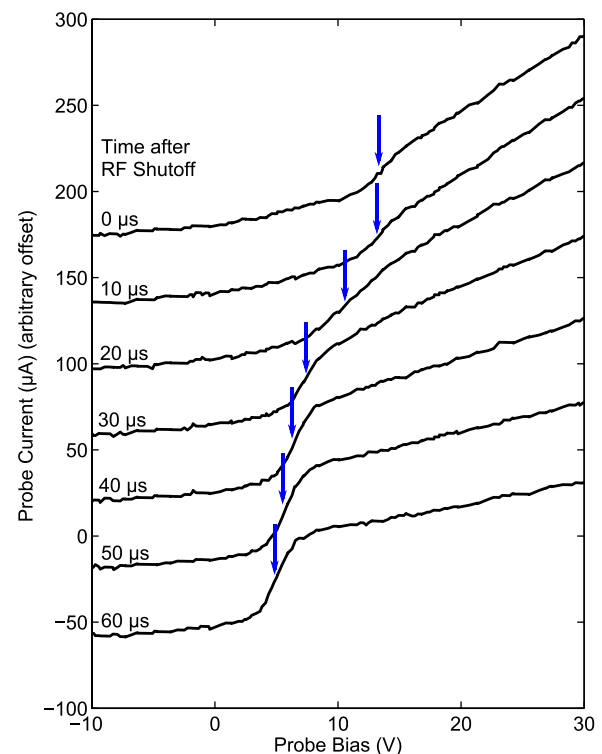


FIG. 4. Emissive probe I-V traces (arbitrary offset) at various times in the afterglow as measured using the slow sweep method. Approximate location of the inflection points are indicated by the arrows.



highly accurate plasma potential measurements to be made in dynamic plasma systems. The temporal resolution is limited by the passive response of the probe (i.e., the RC time constant), which, for our probes, was 10 s of  $\mu\text{s}$ .

## V. MEASUREMENTS IN THE AFTERGLOW

Measurements of the electron temperature were crucial for testing the kinetic emissive sheath theory. The slope of the semilog graph of a Langmuir probe I-V trace is an accurate, well established method for determining the plasma electron temperature,<sup>21</sup> but late in the afterglow when the density and temperature were very low, the low signal to noise ratio made such measurements impossible. To approximate the electron temperature, the floating potential of a non-emitting surface was used<sup>30</sup>

$$T_{ep} \approx \frac{e(V_P - V_{F,EP})}{\ln\left(\frac{\mu}{2\pi}\right)^{\frac{1}{2}}} = \frac{e(V_P - V_{F,EP})}{3.5}, \quad (1)$$

where  $V_P$  is the plasma potential as measured by the emissive probe using the inflection point in the limit of zero emission,  $V_{F,EP}$  is the floating potential of the probe when cold, and  $\mu$  is the ion to electron mass ratio.

The plasma electron temperature approximation was validated by the Langmuir probe technique early in the afterglow where electron temperature could still be extracted. The results are shown in Fig. 5. The agreement between these two techniques is excellent. The major deviation was the first 30  $\mu\text{s}$  of the afterglow, which was caused by the finite decay in the RF signal and capacitive effects in the probe which affected all measurements in those times. Measurements in the first 30  $\mu\text{s}$  were not used in the final analysis. The results of this comparison justify the use of Eq. (1) for measuring the plasma electron temperature in the afterglow.

The cathode's floating potential, the plasma potential, and the electron temperature were measured as a function of time throughout the afterglow when the cathode was cold and not emitting (see Fig. 6). When the RF power was on, all measurements had large fluctuations due to the RF fields. Because the charge densities depend on the ion and electron

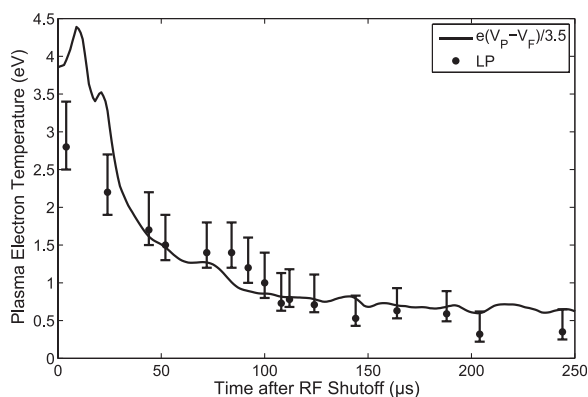


FIG. 5. A comparison of the Langmuir probe measurements to the floating potential measurement of the plasma electron temperature.

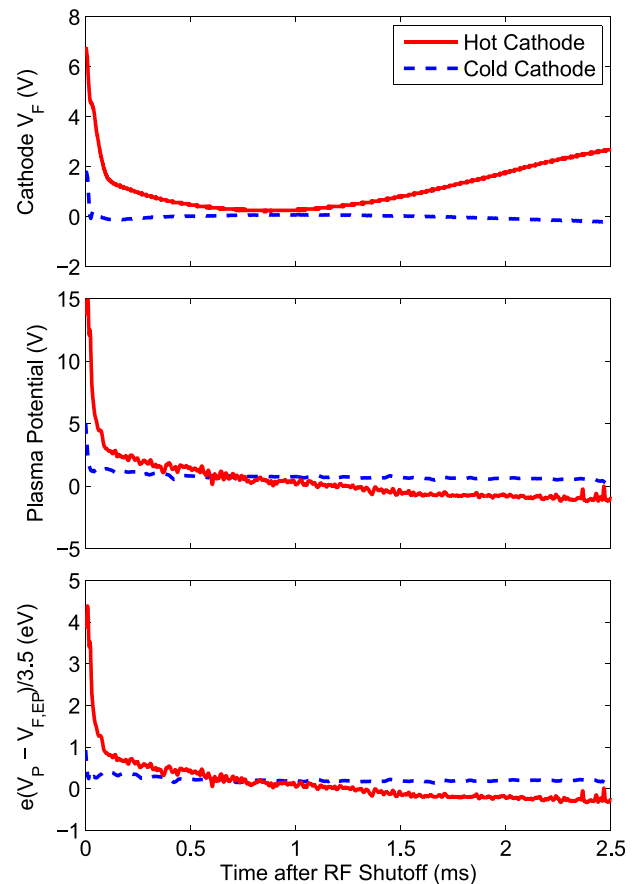


FIG. 6. The floating potential of the cathode, plasma potential, and plasma electron temperature versus time in the afterglow when the cathode was cold and non-emitting (blue dashed lines) and hot and emitting (red solid lines).

sheath transit times, one can expect the sheath dynamics to be complex while the RF was on. After the RF was shut off, the cold cathode potential rapidly decayed to near zero, as expected. The sharp drop and then the brief recovery in the first 20  $\mu\text{s}$  was caused by the capacitive response of the electrode's circuit. The plasma potential decayed rapidly in the first few 10 s of  $\mu\text{s}$  and then slowly thereafter, falling from  $\sim 1$  V to  $\sim 0.5$  V over the course of 2.5 ms. The electron temperature decayed to  $\sim 0.2$  eV at 500  $\mu\text{s}$  and maintained that value for the rest of the afterglow. These decay times are consistent with previous measurements and theories.<sup>26,31,32</sup> The noise in the plasma electron temperature comes principally from the noise in the plasma potential measurement.

The three measured parameters decayed more slowly in the first half millisecond when the cathode was hot and emitting (see Fig. 6). Plasma electrons with energies larger than the emissive sheath potential could reach the cathode surface and be lost, but they were replaced by emitted electrons. This process reduced the number of electrons in the bulk with energies much larger than the emissive sheath potential, but increased the number with energies just slightly larger than the emissive sheath potential. Those emitted electrons provided a source of energy during the afterglow. Because of this effect, the electron temperature decayed more slowly which resulted in the plasma potential decaying more slowly. The cathode floating potential was tied to the plasma potential via the sheath potential, so that

parameter, too, decayed more slowly when the cathode was heated and emitting electrons.

The plasma potential and electron temperature stopped their rapid decay and began decaying more slowly starting  $\sim 100 \mu\text{s}$  into the afterglow, maintaining the decay until the RF power was turned on again at 2.5 ms. The floating potential of the cathode behaved differently, decreasing until time  $870 \mu\text{s}$  and then increasing. Since the cathode was held at a constant temperature, the flux of emitted thermionic electrons was constant, but the flux of plasma electrons decreased as time progressed in the afterglow because the electron temperature and density decayed. A potential barrier between the emitting surface and the virtual cathode minimum, with a potential on the order of the difference between the bulk plasma potential and virtual cathode minimum, formed to suppress the emitted electron flux, causing the cathode floating potential to rise. Eventually, after the plasma electron temperature and density decayed sufficiently, the flux of emitted electrons dominated and significantly altered the discharge. After the floating potential of the cathode began to increase, the plasma potential dropped below ground ( $1150 \mu\text{s}$ ). At this point the estimate of the plasma electron temperature from Eq. (1) is certainly invalid, as it becomes negative. This result provides further evidence that the emitted electrons dominated the discharge in later times, so measurements after  $870 \mu\text{s}$  were not used to evaluate the theory.

Although our measurements indicated that electron emission can change the decay time constant of the plasma potential and electron temperature, we did not study how varying the emitted electron current could allow for control over the time constant. Additionally, the surface area of emitted electrons almost certainly plays a role beyond affecting the emitted electron current as it would significantly affect the plasma electron flux as well. This is a complex system that will need to be considered rigorously in its own right for electron emission to be used to modify bulk parameters.

## VI. PRESHEATH MEASUREMENTS

Early in the afterglow ( $\leq 250 \mu\text{s}$ ), the sheath potential was large enough that meaningful measurements of the presheath potential profile could be made using the inflection point in the limit of zero emission technique (see Fig. 7). The potential was measured as a function of position and time for two emissive limits of the cathode—non-emitting and space-charge limited emission. Two significant observations can be drawn from these data. First, the potential above an emitting surface was consistently lower than that above a non-emitting surface. Second, the sheath potential penetrated further into the plasma by approximately 50% when the cathode was emitting electrons. These two observations lead us to conclude that the emitted electrons reduced the net space-charge which, by Poisson's equation, reduced the electric field and the curvature of the potential. Therefore, the potential drop occurred over a larger distance.

Because of these effects, neither ions nor electrons are accelerated as much in an emissive sheath as in a collecting sheath, but the emissive sheath interacts with a larger volume

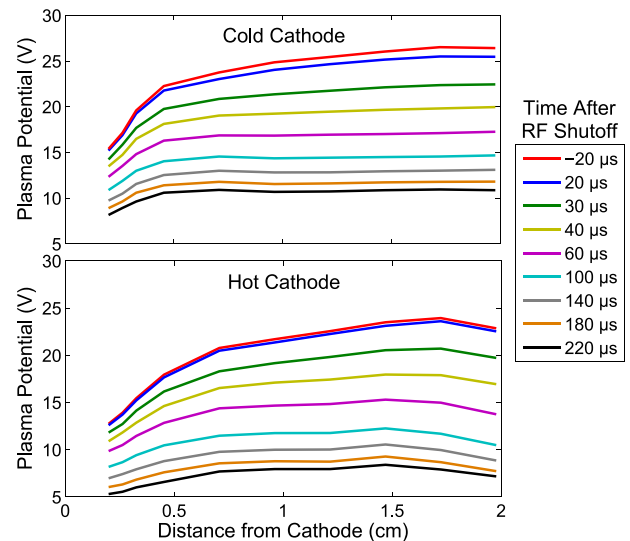


FIG. 7. Potential profiles in the presheath near the cathode when the cathode was cold and not emitting (top) and hot and emitting (bottom) for a variety of times relative to the RF shutoff.

of plasma than the collecting sheath. Ions still need to be accelerated to fulfill Bohm's criterion, so the physical extent of the presheath must be larger than in the collecting case. The emitted electrons modify Bohm's criterion, but only increase the minimum ion energy by  $\sim 5\%$ . In practice, space-charge limited emissive sheath are usually only found surrounding emissive probes, which are small enough that the extended size of the sheath is still insignificant. Near large emitting surfaces, however, such as a large emissive cathode or boundaries with significant secondary electron emission, the extension could play an important role in the system.

## VII. COMPARISON TO KINETIC THEORY

The time from 60 to  $870 \mu\text{s}$  in the afterglow was used to examine the emissive sheath potential. Because the cathode was heated to  $900^\circ\text{C}$  and thermionically emitting electrons, the temperature of the emitted electrons was assumed to be equal to the temperature of the surface:  $\sim 0.1 \text{ eV}$ .<sup>17</sup> To make a comparison to the kinetic theory shown in Fig. 1, the potential difference between the plasma and the floating surface normalized to the plasma electron temperature was graphed versus the ratio of the plasma electron temperature to the emitted electron temperature in Fig. 8.<sup>16</sup> The uncertainty was due principally to the measurement of the plasma potential, which propagated uncertainty to the electron temperature measurement.

As time progressed in the afterglow, the plasma became cooler and cooler, so data shown in Fig. 8 progress from right to left temporally. The predominant feature of the graph is that as the plasma electron temperature approached the emitted electron temperature the floating potential of the planar heated electrode approached the plasma potential. This result supports the predictions made by the kinetic theory. One difference, however, is that the emissive sheath potential was not greatly affected by the electron temperature ratio until that ratio was below about 3. The kinetic theory

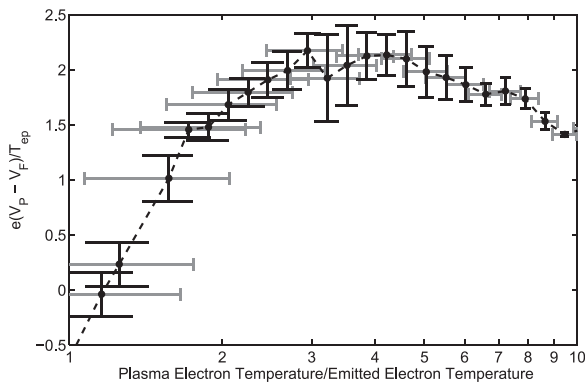


FIG. 8. Measurements of the potential difference between the plasma potential in the bulk and the floating potential of the heated electrode normalized to the plasma electron temperature versus the plasma electron temperature to emitted electron temperature ratio.

predicted that significant change in the emissive sheath potential occurs for ratios less than 100. Additionally, there is a maximum sheath potential when the temperature ratio is between 3 and 5, a result not expected from the theory.

A number of causes of this discrepancy are possible. First, these data were not a direct comparison to the results of the kinetic theory. The kinetic theory predicts the potential difference between the sheath edge potential and the potential minimum of the virtual cathode. Every attempt was made to ensure the potential difference between the surface and the virtual cathode minimum was small, but the emissive sheath still had a presheath. Therefore, it was expected that the measured plasma to floating potential difference would be larger than the sheath potential by the potential of the presheath, a value between  $0.5T_{ep}$  and  $T_{ep}$ .<sup>10,33</sup> No current theories predict how the presheath is affected by electron emission so the presheath's precise potential is unknown.

Although the largest possible cathode was used so the experiment would be relevant to the one dimensional theory, the measurements were made in a fundamentally three dimensional system. It is possible that a radial component of the electric field existed, altering the acceleration of ions and electrons. It is difficult to predict what effect this would have on the sheath potential, but it, too, could be a source of the discrepancy between experiment and theory.

The kinetic theory assumed that no instabilities were present in the emissive sheath, so sheath instabilities in the measurements could be the cause of the discrepancy. The particle-in-cell simulations that validated the kinetic theory observed disruptive ion acoustic instabilities if the simulation space was too large. These instabilities may significantly affect the time averaged sheath potential, though a detailed investigation into emissive sheath instabilities is beyond the scope of this work.

## VIII. CONCLUSIONS

Measurements of the plasma potential and plasma electron temperature were made in the afterglow of a capacitively coupled RF plasma. The slow-sweep probe method<sup>26–28</sup> was used in conjunction with the inflection point in the limit of zero emission emissive probe technique<sup>22</sup> to

obtain emissive probe I-V traces as a function of time. This is the first time that the inflection point technique was used to make time-resolved plasma potential measurements, a great asset for this method, which is the most accurate of the emissive probe techniques.<sup>2,8</sup> These measurements showed that the electron temperature and plasma potential decay more slowly when an emissive cathode was present in the chamber. This can be attributed to the energy deposited by the influx of electrons from the heated cathode. Using an electron source in an RF plasma, it may be possible to control the rate at which the plasma potential and electron temperature decay in the afterglow.

The potential profile in the presheath as a function of time relative to the RF shutoff was also measured. The plasma potential above an emitting surface was lower than that above a non-emitting surface and the sheath potential penetrated further into the plasma. The emitted electrons reduced the net space-charge which reduced the electric field and the curvature of the plasma potential. By controlling the emissive properties of plasma facing surfaces, one can modify the plasma boundary and the bulk plasma parameters, though further study is needed to understand this coupling.

Measurements of the emissive sheath potential in the afterglow confirmed kinetic theory predictions that the sheath potential shrinks when the plasma electron temperature approaches the emitted electron temperature and disappears entirely when those two temperatures are equal. When the plasma electron temperature was much larger than the emitted electron temperature, the normalized potential difference between the floating potential of a highly emitting planar surface and the plasma potential was independent of the electron temperature. As the plasma electron temperature dropped later in the afterglow, it became low enough ( $T_{ep} \lesssim 3T_{ee}$ ) the plasma electron temperature to emitted electron temperature ratio greatly affects the sheath potential, reducing that potential as  $T_{ep} \rightarrow T_{ee}$ . The effect of the emissive sheath potential going to zero when the plasma electron temperature equals the emitted electron temperature was experimentally verified. For intermediate ratios ( $T_{ep} \sim 5T_{ee}$ ), the potential difference was larger than expected.

## ACKNOWLEDGMENTS

This work was supported by US Department of Energy Grant No. DE-FG02-97ER54437, the DOE Office of Fusion Energy Science Contract No. DE-SC0001939, and the Fusion Energy Sciences Fellowship Program administered by Oak Ridge Institute for Science and Education under a contract between the U.S. Department of Energy and the Oak Ridge Associated Universities.

<sup>1</sup>D. Sydorenko, I. Kaganovich, Y. Raitses, and A. Smolyakov, *Phys. Rev. Lett.* **103**, 145004 (2009).

<sup>2</sup>J. P. Sheehan and N. Hershkowitz, *Plasma Sources Sci. Technol.* **20**, 063001 (2011).

<sup>3</sup>P. J. Harbour and M. F. A. Harrison, *J. Nucl. Mater.* **76–77**, 513 (1978).

<sup>4</sup>G. D. Hobbs and J. A. Wesson, *Plasma Phys.* **9**, 85 (1967).

<sup>5</sup>W. Li, J. X. Ma, J.-J. Li, Y.-B. Zheng, and M.-S. Tan, *Phys. Plasmas* **19**, 030704 (2012).

- <sup>6</sup>T. Intrator, M. H. Cho, E. Y. Wang, N. Hershkowitz, D. Diebold, and J. Dekock, *J. Appl. Phys.* **64**, 2927 (1988).
- <sup>7</sup>R. F. Kemp and J. M. Sellen, *Rev. Sci. Instrum.* **37**, 455 (1966).
- <sup>8</sup>J. P. Sheehan, Y. Raiteses, N. Hershkowitz, I. Kaganovich, and N. J. Fisch, *Phys. Plasmas* **18**, 073501 (2011).
- <sup>9</sup>D. Bohm, in *The Characteristics of Electrical Discharges in Magnetic Fields*, edited by A. Guthrie and R. K. Wakerling (McGraw-Hill, New York, 1949), pp. 77–86.
- <sup>10</sup>K. U. Riemann, *J. Phys. D: Appl. Phys.* **24**, 493 (1991).
- <sup>11</sup>M. Y. Ye and S. Takamura, *Phys. Plasmas* **7**, 3457 (2000).
- <sup>12</sup>T. Gyergyek and M. Cercek, *Contrib. Plasma Phys.* **45**, 89 (2005).
- <sup>13</sup>L. A. Schwager, *Phys. Fluids B* **5**, 631 (1993).
- <sup>14</sup>L. A. Schwager, W. L. Hsu, and D. M. Tung, *Phys. Fluids B* **5**, 621 (1993).
- <sup>15</sup>J. P. Sheehan and N. Hershkowitz, *J. Vac. Sci. Technol. A* **30**, 031302 (2012).
- <sup>16</sup>J. P. Sheehan, N. Hershkowitz, I. D. Kaganovich, H. Wang, Y. Raiteses, E. V. Barnat, B. R. Weatherford, and D. Sydorenko, *Phys. Rev. Lett.* **111**, 075002 (2013).
- <sup>17</sup>C. Herring and M. H. Nichols, *Rev. Mod. Phys.* **21**, 185 (1949).
- <sup>18</sup>H. Seiler, *J. Appl. Phys.* **54**, R1 (1983).
- <sup>19</sup>P. J. Hargis, K. E. Greenberg, P. A. Miller, J. B. Gerardo, J. R. Torczynski, M. E. Riley, G. A. Hebner, J. R. Roberts, J. K. Olthoff, J. R. Whetstone, R. J. Vanbrunt, M. A. Sobolewski, H. M. Anderson, M. P. Splichal, J. L. Mock, P. Bletzinger, A. Garscadden, R. A. Gottscho, G. Selwyn, M. Dalvie, J. E. Heidenreich, J. W. Butterbaugh, M. L. Brake, M. L. Passow, J. Pender, A. Lujan, M. E. Elta, D. B. Graves, H. H. Sawin, M. J. Kushner, J. T. Verdeyen, R. Horwath, and T. R. Turner, *Rev. Sci. Instrum.* **65**, 140 (1994).
- <sup>20</sup>J. K. Olthoff and K. E. Greenberg, *J. Res. Natl. Inst. Stand. Technol.* **100**, 327 (1995).
- <sup>21</sup>N. Hershkowitz, in *Plasma Diagnostics*, edited by O. Auciello and D. L. Flamm (Academic Press, Inc., New York, 1989), Vol. 1, pp. 113–183.
- <sup>22</sup>J. R. Smith, N. Hershkowitz, and P. Coakley, *Rev. Sci. Instrum.* **50**, 210 (1979).
- <sup>23</sup>L. Giannone, R. Balbin, H. Niedermeyer, M. Endler, G. Herre, C. Hidalgo, A. Rudyj, G. Theimer, and P. Verplanke, *Phys. Plasmas* **1**, 3614 (1994).
- <sup>24</sup>G. Chiodini, C. Riccardi, and M. Fontanesi, *Rev. Sci. Instrum.* **70**, 2681 (1999).
- <sup>25</sup>R. B. Lobbia and A. D. Gallimore, *Phys. Plasmas* **17**, 073502 (2010).
- <sup>26</sup>A. Maresca, K. Orlov, and U. Kortshagen, *Phys. Rev. E* **65**, 056405 (2002).
- <sup>27</sup>J. T. Gudmundsson, J. Alami, and U. Helmersson, *Surf. Coat. Technol.* **161**, 249 (2002).
- <sup>28</sup>C. S. Yip, J. P. Sheehan, N. Hershkowitz, and G. Severn, *Plasma Sources Sci. Technol.* **22**, 065002 (2013).
- <sup>29</sup>J. W. Bradley, H. Backer, P. J. Kelly, and R. D. Arnell, *Surf. Coat. Technol.* **142–144**, 337 (2001).
- <sup>30</sup>D. Staack, Y. Raiteses, and N. J. Fisch, *Appl. Phys. Lett.* **84**, 3028 (2004).
- <sup>31</sup>R. R. Arslanbekov and A. A. Kudryavtsev, *Phys. Rev. E* **58**, 7785 (1998).
- <sup>32</sup>Y. Celik, T. V. Tsankov, M. Aramaki, S. Yoshimura, D. Luggenhoelscher, and U. Czarnetzki, *Phys. Rev. E* **85**, 046407 (2012).
- <sup>33</sup>L. Oksuz and N. Hershkowitz, *Phys. Rev. Lett.* **89**, 145001 (2002).